The Journal of Chemical Physics

RESEARCH ARTICLE | FEBRUARY 21 2024

# Supersaturation dependent nucleation of methane + propane mixed-gas hydrate

**Special Collection:** Porous Solids for Energy Applications

Tsutomu Uchida ; Ren Sugibuchi; Masato Hayama; Kenji Yamazaki



*J. Chem. Phys.* 160, 074502 (2024)
https://doi.org/10.1063/5.0189967







AIP Publishing

The Journal of Chemical Physics ARTICLE pubs.aip.org/aip/jcp

# Supersaturation dependent nucleation of methane + propane mixed-gas hydrate

Cite as: J. Chem. Phys. 160, 074502 (2024); doi: 10.1063/5.0189967
Submitted: 1 December 2023 • Accepted: 28 January 2024 •
Published Online: 21 February 2024



Tsutomu Uchida,[1,a)] Ren Sugibuchi,[2] Masato Hayama,[2] and Kenji Yamazaki[1]

## AFFILIATIONS

[1] Division of Applied Physics, Faculty of Engineering, Hokkaido University, Sapporo 060-8628, Japan
[2] Division of Applied Physics, Graduate School of Engineering, Hokkaido University, Sapporo 060-8628, Japan

**Note:** This paper is part of the JCP Special Topic on Porous Solids for Energy Applications.
[a)] **Author to whom correspondence should be addressed:** t-uchida@eng.hokudai.ac.jp

## ABSTRACT

Before hydrates can be widely used in industry, we should better understand the problematic issues of hydrate nucleation, particularly its stochastic nature. Here, we report on measurements of the nucleation probability of mixed-gas hydrates in which the guest molecules are a mixture of methane and propane. For the pure cases, at a supersaturation near 1.0, we had previously measured an induction time for the methane hydrate of about 1 h, whereas for the propane hydrate, it was over one day. Using the same experimental setup, we examine here the nucleation probability for a mixture of 90% methane and 10% propane as the guest gas for a range of supersaturations. For the experiments, the temperature was 274 ± 0.5 K and the stirring rate was about 300 rpm. The experiments were repeated at least ten times under the same condition, exchanging the sample water every time. We define the nucleation probability at a given time as the fraction of trials that nucleated by that time and then determine the nucleation probability distribution. The resulting nucleation frequency is found to have a power-law relation to supersaturation. Then, we examine how the nucleation frequency is affected by the existence of ultrafine bubbles in the initial water. We find that the ultrafine bubbles increase the nucleation frequency but much less than that of typical changes in supersaturation.





## I. INTRODUCTION

Gas hydrates are expected to be used as a functional material for the transport and storage of natural gas. However, for any such application, we must first develop technology to efficiently form gas hydrates from natural gas. The formation problem is twofold. Gas hydrates form via two processes: first, nucleation occurs after a sometimes lengthy induction period; next is the bulk growth period, which can also be time-consuming. To date, the focus of most hydrate experimental studies has been on the growth processes,[1–16] with relatively few studies on hydrate nucleation.[3,4,9,11,15–20]

As nucleation of gas hydrates from gas and water requires supersaturation (supercooling), various methods have been investigated to promote their formation, including trials of different mixing operations, using various additives, and methods to use the "memory effect," which shortens the induction period when using the hydrate-dissociated water.[21] However, their quantitative evaluations are difficult because the stochastic nature of nucleation requires multiple experiments to demonstrate a statistical superiority of any proposed method.

Previously, Natarajan *et al.*[17] measured the induction time ($t_{ind}$) of methane ($CH_4$), ethane ($C_2H_6$), and carbon dioxide ($CO_2$) hydrates. They found that $t_{ind}$ had a power-law dependence on the supersaturation with a particularly large increase at low supersaturations. Uchida *et al.*[21–24] measured the variation in induction times of several nucleation-promoting methods for single-gas hydrates [$CO_2$, $CH_4$, $C_2H_6$, and propane ($C_3H_8$)] to obtain nucleation probability distributions. In particular, for $CH_4$ and $C_3H_8$, which are the main components of natural gas, the induction time for the $C_3H_8$ hydrate was about ten times longer than that for the $CH_4$ hydrate. All methods involved using a high-pressure vessel with a stirrer, and $t_{ind}$ was defined as the time period where no nucleation events (turbidity, temperature rise, or pressure drop) occur under the formation condition. Those studies showed that the nucleation probability distribution varies with the gas species. Although there is still some debate about whether or not the nucleation occurs very early in the induction period,[25] we assume here that the measurable nucleation events and the observed crystal growth occur soon after the first nucleation in the gas–water system, and thus, the variation in $t_{ind}$ must relate to the nucleation probability.

In addition, Uchida *et al.*[21–24,26] performed similar experiments by changing the source water from pure water, hereafter PW, to either gas-hydrate dissociated water, hereafter DW, or water containing ultrafine bubbles (UFBs), hereafter UW, and investigated how the change of source water affects the nucleation probability distribution of gas hydrates. They found that the "memory effect" occurs not only with DW but also with UW, even though UW has not experienced any gas-hydrate or ice structures. They also used two methods to measure UFBs in both DW and UW, finding roughly the same amount of UFBs in both DW and UW.[21–24,26] These results indicate that the presence of UFBs in water is important for the expression of the "memory effect."

To date, research on gas-hydrate nucleation has been mostly limited to that on pure component gas hydrates.[20] Nevertheless, a few studies with mixed gases have been done. For example, Sloan and Fleyfel[27] analyzed the data on $CH_4 + C_2H_6$ (composition ratio 90:10) taken by Falabella[28] and determined that this system had almost no $t_{ind}$ from the ice + vapor system (183 K and 0.101 MPa). Running another set of experiments on the same guest system, Skovborg *et al.*,[29] instead, measured a $t_{ind}$ of 1–2.5 h in the water + vapor system (274.95 K and 2.05 MPa). In addition, de Menezes *et al.*[30] performed relatively high-pressure experiments (high supersaturation; around 300 K and 60 or 13 MPa) using the isochoric method on $CH_4 + C_3H_8$ (composition ratio 92:8). Although they did not report on $t_{ind}$, we estimate here that the values were close to 45 min.

For this study, we ran experiments on the formation of $CH_4$ and $C_3H_8$ mixed-gas hydrate. Here, we investigate how the nucleation probability distribution compares to those of each single-gas hydrate and how it depends on the initial supersaturation (controlled via the initial pressure). We also examine additional experiments using DW and UW instead of PW to better understand how UFBs affect the nucleation probability of the mixed gas-hydrate. This is the first known study of the nucleation of mixed gas-hydrates that also examine the effect of UFBs.

## II. EXPERIMENTAL PROCEDURES

We used a gas mixture of $CH_4$:$C_3H_8$ = 90:10 from Air Water Hokkaido Inc. (Hokkaido, Japan). According to the CSMHYD program,[31] the equilibrium pressure $P_d$ of the mixed-gas hydrate with this composition at temperature $T$ = 274 K is $P_d$ = 0.55 MPa. With this mixture, we examine the effect of the initial pressure $P_0$ on the induction time $t_{ind}$, with $P_0$ in the range of 1.1–2.5 MPa, giving an initial supersaturation $\sigma = P_0/P_d - 1$ of 1.0–3.5. This range was selected such that the partial pressure of $C_3H_8$ remained lower than its saturation pressure at 274 K.

The source water is PW, having an electrical resistivity of 15 MΩ cm, which is the same as that used in our previous studies. To make a solution of ultrafine bubbles (UFBs), UW, we aerate PW with the mixed-gas source using a UFB generator (Aura Tec, Fukuoka, Japan, type OM4-MDG-045) at a pressure of 250 kPa and a temperature of 293 K, circulating for 1 h. In addition, we prepare hydrate dissociated water (DW), by dissolving some pieces of mixed-gas hydrates (~10 g) that had formed from the same mixed gas and recovered under atmospheric pressure at a temperature below 170 K, in 50 $cm^3$ of PW at room temperature. These preparations are the same as those of our previous studies for single-gas hydrates.[21–24] To reduce the effect of surface UFBs on the vessel wall, which may form after introducing the UFB-containing water, we store the liquid sample at room temperature until the sample is free of visible bubbles (at least 1 h) prior to its use in the experiments.

The average diameter and number density of UFBs in these UFB-containing water samples (UW and DW) are evaluated using the same particle tracking analysis method (NanoSight, Quantum Design Japan, Tokyo, Japan, type NS500, λ = 635 nm) as we used in previous studies.[21–24] In this method, a device records the movement of UFBs, and then, the motion is analyzed to determine each UFB's size using the Stokes–Einstein equation. Using this system, we can measure the UFBs having diameters of 50–300 nm. As several tens of UFBs are typically observed in a frame, we can obtain the size distributions and the number density of UFBs. The averaged values for the UFB distribution are estimated from at least six measurements for a specified liquid sample.

The experimental setup is the same as that used for single-gas hydrate formation.[21–24] A high-pressure vessel (232.2 $cm^3$ in volume) equipped with a stirrer is submerged in a constant temperature bath to maintain an experimental temperature at 274 ± 0.5 K. After introducing about 50 $cm^3$ of sample water, $CH_4 + C_3H_8$ mixed gas is added and pressurized to $P_0$. The gas-hydrate formation tests begin at $t$ = 0 with a gentle agitation of about 300 rpm. The temperature and pressure are measured using a data logger every 10 s, and the induction time ($t_{ind}$) is defined as the time difference between the starting time of agitation and the nucleation time $t_f$ (defined this way, the induction and nucleation times are equal). Such nucleation is determined when either the temperature rises or the pressure drops due to the subsequent growth of gas hydrate. When no such nucleation occurs within 9 h (540 min), we mark the case as "no generation."

We repeat each experiment at least ten times under the same conditions, exchanging the fresh source water every time. For a given $t_{ind}$, the fraction of trials that nucleate within this time is the nucleation probability. The cumulative $t_{ind}$ curve is the nucleation probability distribution $\Pi(t)$, which is fitted to Eq. (1)[32,33] using commercially supplied software (Origin Pro 9.0, Light Stone),

$$\Pi(t) = 1 - \exp\left[-J(t - \tau_0)\right], \tag{1}$$

where $J$ is the nucleation frequency and $\tau_0$ is the offset time. Generally, $J$ is closely related to the nucleation rate and $\tau_0$ generally scales with the minimum induction time.

In addition to the estimation of these parameters, we also measure the nucleation promotion effect of UW and DW by determining the total shift of $\Pi(t)$ upon using UW or DW, denoted as $\langle \Delta t_{ind} \rangle$. To determine this shift, we follow the same procedure used in Uchida *et al.*[21,22] This parameter is defined as positive when the induction time is shorter than that for the corresponding pure-water case.

## III. RESULTS AND DISCUSSION

### A. Nucleation probability distributions of mixed-gas and single-gas hydrates

First, we consider the case of a single supersaturation of $\sigma$ = 1.0, looking at the mixed-gas case as well as the single-gas cases. For the mixed-gas case ($CH_4 + C_3H_8$) at $T$ = 274.2 K and $P_0$ = 1.1

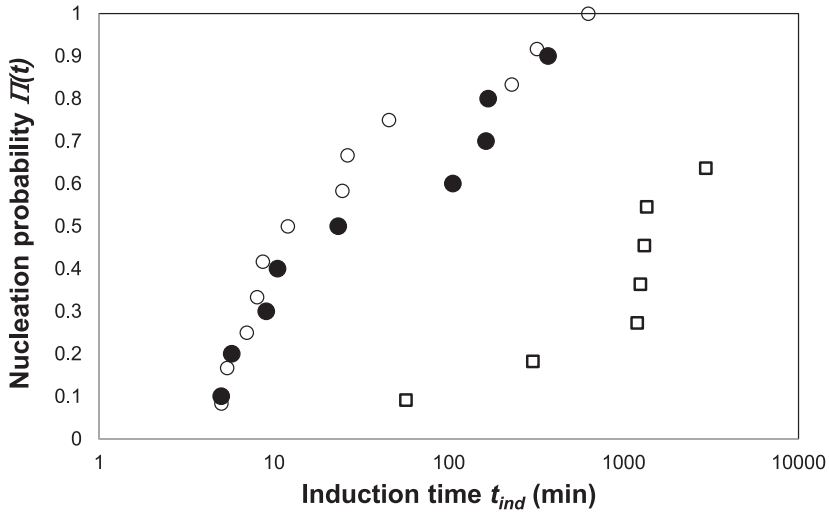


**FIG. 1.** Nucleation probability distribution of the $CH_4 + C_3H_8$ (90:10) mixed-gas hydrate $\Pi(t)$ (marked with •) by the indicated induction time $t_{ind}$, as well as those for pure $CH_4$ hydrate (○, $\sigma = 0.7$)[21] and pure $C_3H_8$ hydrate (□, $\sigma = 1.0$).[23]

MPa ($\sigma = 1.0$), we ran the experiment ten times. Nucleation occurred nine times with $t_{ind}$ varying between 5 and 370 min (one run exhibited "no generation" as defined above).

The $t_{ind}$ results are plotted in Fig. 1. We also show, for comparison, the corresponding curves for the $CH_4$ hydrate[21] when $\sigma = 0.7$ and for the $C_3H_8$ hydrate[23] when $\sigma = 1.0$. (Note here that the supersaturation for the $CH_4$-hydrate experiment is smaller than 1.0.) This figure shows that the nucleation probability distribution of the $CH_4 + C_3H_8$ mixed-gas hydrate is shifted to significantly shorter times than that of the $C_3H_8$ hydrate, whereas it mostly overlaps with the curve of the $CH_4$ hydrate. Although the formation conditions (e.g., $P_0$) are different, the driving force for the hydrate formation is roughly the same. Given that the crystal structure of the mixed-gas hydrate here is thought to be the sII structure,[31] which is the same as that for the single $C_3H_8$ hydrate, the significantly shorter times for the mixed-gas case are not due to the difference in crystal structure. Therefore, the main cause of these differences is likely connected to the composition condition.



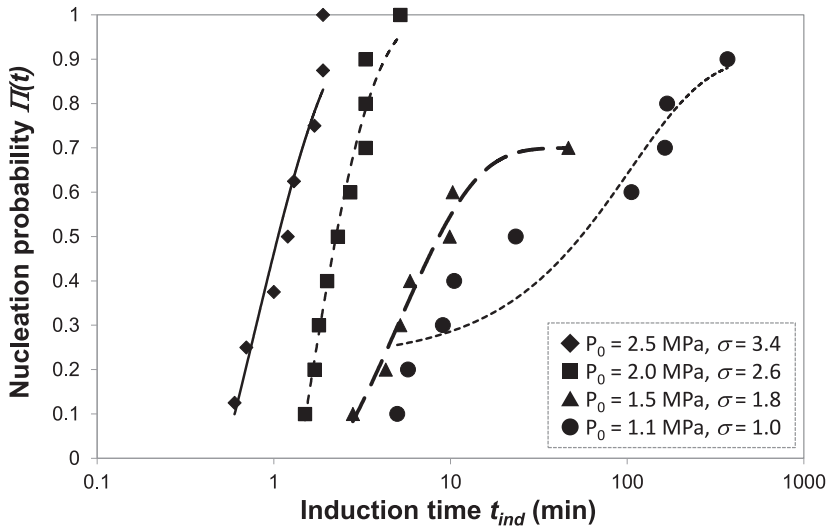


**FIG. 2.** Nucleation probability distribution of the $CH_4 + C_3H_8$ (90:10) mixed-gas hydrate $\Pi(t)$ at four supersaturation $\sigma$ values corresponding to the four initial setting pressures $P_0$ in the legend. The fitting curves are based on Eq. (1).

**TABLE I.** Experimental conditions for each curve in Fig. 2 and the resulting fitting parameters to Eq. (1). The uncertainties are the standard fitting errors.

| $P_0$ (MPa) | $T$ (K) | $\sigma$ | $J$ (min$^{-1}$) | $\tau_0$ (min) | $t_{ind\,(\Pi=0.5)}$ (min) |
|---|---|---|---|---|---|
| 2.5 | 274 | 3.5 | 1.29 ± 0.19 | 0.52 ± 0.07 | 1.06 |
| 2.0 | 274 | 2.6 | 0.80 ± 0.08 | 1.39 ± 0.06 | 2.25 |
| 1.5 | 274 | 1.7 | 0.19 ± 0.02 | 2.15 ± 0.33 | 5.72 |
| 1.1 | 274 | 1.0 | 0.06 ± 0.03 | 0.93 ± 3.38 | 12.6 |

## B. Supersaturation dependence of nucleation probability in mixed-gas hydrates

We now examine how changing the driving force of the crystal-growth process, the supersaturation $\sigma$, affects the nucleation probability distribution of the $CH_4 + C_3H_8$ mixed gas hydrate. Figure 2 shows the nucleation probability distribution when the formation temperature is fixed at 274 K and the supersaturation $\sigma$ increases from 1.0 to 3.5. The supersaturation values represent the initial pressures $P_0$ from 1.1 to 2.5 MPa. The data are fit to Eq. (1) (showing in various lines) and show that the larger the $\sigma$ (higher $P_0$), the shorter the $t_{ind}$, and the narrower the nucleation probability distribution. Thus, as $\sigma$ increases, the nucleation frequency $J$ increases.

Table I lists the nucleation frequency $J$ and offset time $\tau_0$ for the data in Fig. 2 as calculated by fitting to Eq. (1). When $\sigma$ is 1.0, the value of $J$ is similar to the nucleation frequency of single-gas hydrate ($\sim 10^{-2}$ min$^{-1}$). Increasing $\sigma$ by a factor of 2 to 3 increases $J$ by a factor of over 10. Meanwhile, the value of $\tau_0$ decreases by a factor of about 2 to 4 over the same increase in supersaturation.

For a single-gas hydrate, Natarajan *et al.*[17] derived an empirical equation from crystal growth theory that shows that the value $t_{ind}$ decreases with increasing supersaturation $\sigma$ as $t_{ind} = K\,\sigma^{-m}$, where K and m are constants. For the $CH_4$ hydrate, they obtained K = 5.194 min and m = 1.21. Their study expressed supersaturation not in terms of pressure, as we do here, but in terms of fugacity. Another difference between their study and ours is the range of supersaturation: we use larger supersaturations ($\sigma$ up to 3.5) than their study ($\sigma < 1.1$). To compare our results with the previous study, we estimate the typical $t_{ind}$ for each $\sigma$ as the time until $\Pi = 0.5$ in Eq. (1) (shown in the last column of Table I) and find that they also have a power-law dependence, specifically $t_{ind(\Pi=0.5)} = K\,\sigma^{-m}$. Although both of our fitting parameters (K = 14.4 min and m = 2.0) are larger than those estimated in the previous study, we confirm that $t_{ind}$ has a power-law relation to $\sigma$ in the range we studied.

Natarajan *et al.*[17] also show that an increase in supersaturation decreases the variability. This is consistent with our finding that an increase in $\sigma$ increases the nucleation frequency $J$ (Table I). The previous models[17–19] suggest that $J$ has a power-law relation to $\sigma$ as

$$J = k\,\sigma^{n}, \tag{2}$$

where k and n are constants. As a test, we fit our data in Fig. 3 to Eq. (2), finding that $k = 5.5 \times 10^{-2}$ and n = 2.6. The good fit suggests that this hydrate system is consistent with the previous models.[17–19]

Using a mixed gas of $CH_4 + C_2H_6$ (composition ratio 90:10), Skovborg *et al.*[29] reported that $t_{ind}$ was observed in the water–vapor system, yet Sloan and Fleyfel[27] observed no $t_{ind}$ in the ice–vapor system. Natarajan *et al.*[17] explained this difference to be due to the difference in the driving force. This means that if the driving force is sufficiently large, $t_{ind}$ is not observed, whereas if the driving force is small, $t_{ind}$ can be observed and its variation tends to be large. In the case where $t_{ind}$ was observed in the water–vapor system,[29] the supersaturation degree $\sigma$ was estimated to be about 0.1, based on the equilibrium pressure of 1.87 MPa at the experimental temperature (CSMHYD[31]). In contrast, Natarajana *et al.*[17] suggested that the supersaturation degree $\sigma$ in the ice–vapor system[27] was more than 7. Our study here uses a different mixed gas and middling supersaturations, yet at our lowest supersaturation value of $\sigma \sim 1$, we also find that $t_{ind}$ ranges from several minutes to 6 h. Therefore, we confirmed that the nucleation phenomenon under low supersaturations tends to exhibit strong stochastic characteristics in the formation of mixed-gas hydrates, at least in the water–vapor system.

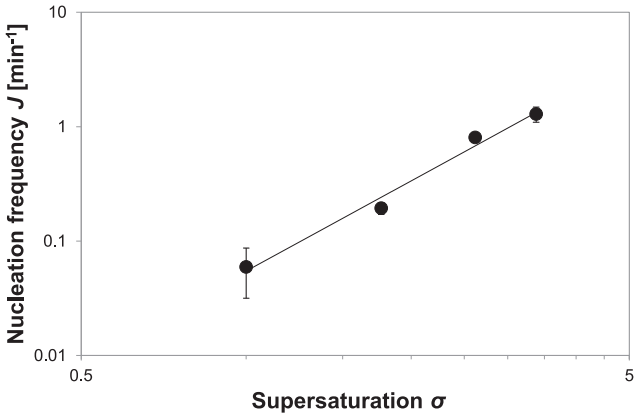


**FIG. 3.** Nucleation frequency $J$ estimated from the nucleation probability distribution of the $CH_4 + C_3H_8$ (90:10) mixed-gas hydrate (Fig. 2) for a range of supersaturations $\sigma$. The error bars show the standard error of fitting of Eq. (1). The solid line shows the fit to Eq. (2).

To check the disappearance of $t_{ind}$ under higher supersaturation conditions, we analyze the experimental data of a previous study that used the similar mixed gas. de Menezes *et al.*[30] performed experiments on the $CH_4 + C_3H_8$ (composition ratio 92:8) mixed-gas hydrate under stirring conditions using the isochoric method, but with a much higher supersaturation of about 10.7 (calculated from the initial pressure). The initial conditions were 15 MPa and 312.7 K for four experiments. As the temperature decreased, the hydrate formed at about 278.3 K all four times. Based on the numerical data of these experiments,[34] we estimated the $t_{ind}$ values (the time until hydrate formation after crossing into equilibrium conditions) and find that they are narrowly distributed in the range of 43.5–47.3 min. (The uncertainty of this range comes from the ±0.2 min time interval of measurement.) From Eq. (2), $J = 26.1$, a high nucleation frequency that suggests that there should be almost no variation in $t_{ind}$, as observed. However, according to Natarajan *et al.*,[17] the value of $t_{ind}$ should essentially be zero for such a large $\sigma$. Therefore, the values of $t_{ind}$ are consistent with experiments at lower pressures, whereas the small dispersion of values is consistent with other experiments at higher supersaturations. So, the induction period itself may not

be decided by supersaturation only, but also depend on other factors (e.g., absolute temperature and the experimental procedures).

In classical nucleation theory, as applied to gas hydrates, the radius of the critical nucleus $R^*$ and the Gibbs free energy barrier for the formation of a critical nucleus $\Delta G(R^*)$ depend on the chemical potential difference $\Delta\mu$ as[17–19,35]

$$R^* = 2\,\gamma v_H/\Delta\mu \tag{3}$$

and

$$\Delta G(R^*) = \frac{16}{3}\Pi v_H^2 \frac{\gamma^3}{\Delta\mu^2}, \tag{4}$$

where $\gamma$ is the liquid–solid (hydrate) interfacial tension and $v_H$ is the volume of a hydrate building unit. Here, $\Delta\mu$ is the chemical potential difference of water and guest molecules, which is given by the following equation:[3,4]

$$\Delta\mu = \Delta\mu_g + n_w\,\Delta\mu_w, \tag{5}$$

where $\Delta\mu_g$ is the chemical potential difference of guest molecules from equilibrium conditions, $n_w$ is the hydration number, and $\Delta\mu_w$ is the chemical potential difference of water molecules. Here, we assume that $\gamma$ is equal to that of ice in water and $v_H$ is given by the small cage volume (one guest molecule and $n_w$ water molecules). Since $\Delta\mu$ is proportional to the driving force of nucleation $\Delta P = P_0 - P_d$, or equivalently $\sigma$, these equations show that the larger the $\sigma$ is, the smaller the $R^*$ and the lower the $\Delta G(R^*)$ become and, thus, the easier that nucleation occurs. For the isothermal formation process of the $CH_4$ hydrate, Kashchiev and A. Firoozabadi[18,19] suggested that $J$ increases and $t_{ind}$ decreases exponentially with $\Delta P$ because Eqs. (3)–(5) show that $R^*$ and $\Delta G(R^*)$ decrease when $\Delta P$ increases. Our results here qualitatively support these previous findings.

### C. Variation in nucleation probabilities with different water samples

Previous studies showed that hydrate nucleation is promoted when pure source water is replaced with that containing UFBs.[21] We tested this effect here for the case of mixed-gas hydrates.

The source water was either the hydrate-dissociated water (DW) or the UFB-containing water (UW) prepared using a UFB generator. These samples had $10^7$ to $10^8$ UFBs/ml with an average diameter of 100–200 nm. The gas used for generating UFBs and for gas-hydrate formation was the same $CH_4 + C_3H_8$ mixture ($CH_4$:$C_3H_8$ = 90:10). The gas-hydrate formation temperature and pressure were 274 K and 1.1 MPa ($\sigma$ = 1.0), the same as those used for the PW sample. The $t_{ind}$ value was measured ten times, each time with fresh sample water.

As shown in Fig. 4, both probability distributions with DW and UW shift to shorter times compared to that with PW. Therefore, the results confirm that UFBs have a nucleation-promoting effect even on the mixed-gas hydrate formation.

Table II shows the results of fitting the data in Fig. 4 to Eq. (1). Compared to the results with PW, the nucleation rate $J$ increases by a factor of 1.2 for DW and by a factor of 1.4 for UW. In addition, the expected shift in induction time $\langle\Delta t_{ind}\rangle$, which indicates the degree of nucleation promotion over PW, exceeds 20 h. Thus, the results

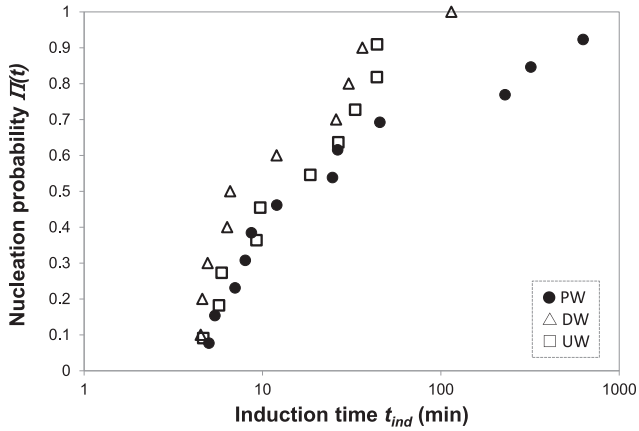


**FIG. 4.** Nucleation probability distribution of the $CH_4 + C_3H_8$ (90:10) mixed-gas hydrate $\Pi(t)$ using either UFB-containing water (DW: △ and UW: □) or pure water (●). All were run under conditions with $\sigma$ = 1.0.

**TABLE II.** Fits of the nucleation probability distributions of Fig. 4 to Eq. (1). The uncertainties are the standard fitting errors.

| | $J$ ($\times 10^{-2}$ min$^{-1}$) | $\tau_0$ (min) | $\langle\Delta t_{ind}\rangle$ (min) |
|---|---|---|---|
| Pure water (PW) | 5.9 ± 2.8 | 0.9 ± 3.4 | ··· |
| Dissociated water (DW) | 6.8 ± 1.1 | 1.9 ± 1.4 | 1247 |
| UFB water (UW) | 8.0 ± 1.1 | −0.5 ± 0.9 | 1227 |

show that this mixed-gas hydrate has a nucleation-promoting effect from UFB-containing waters.

We now compare these increases in $J$ to those found earlier for the single-gas cases. Earlier, we found that the value of $J$ for the $CH_4$ hydrate was 1.1 times larger for DW and 1.6 times larger for UW at $\sigma$ = 0.7.[21] In the case of $C_3H_8$ hydrate, at $\sigma$ = 1.0, we found that $J$ was 2.9 times larger for DW and 5.1 times larger for UW.[23] Thus, the mixed-gas hydrate obtained here has increases closer to those found previously for the $CH_4$ hydrate. This result may be due to the gas composition here being $CH_4$-rich. In future studies, we plan to examine different compositions to help clarify the effect.

Next, we compare the UFB influence on $J$ to the $\sigma$ dependence of $J$, which was found in the pure water system. Figure 5 shows that the promotion effect of UFBs on $J$ is much smaller than its $\sigma$ dependence. In particular, the promotion effect of UFBs is equivalent to only about a 9%–16% increase in $\sigma$.

Theoretically, UFBs may affect hydrate nucleation by providing new nucleation sites (proportional to the vapor–liquid interface area) or by providing a buffer of guest molecules that locally maintain a relatively high supersaturation in the liquid phase.[21] Which is the likely mechanism in our study? If the UFBs act as a hydrate nucleation site, nucleation becomes heterogeneous. Assuming that we have an average UFB diameter of 200 nm and a number density of $10^8$ UFBs/ml, the total UFB vapor–liquid interface area in our experiments is of order $10^{-1}$ cm$^2$/ml. Based on model estimates,[3,4,17–19] the value of γ would change in Eqs. (3) and (4) such as to decrease

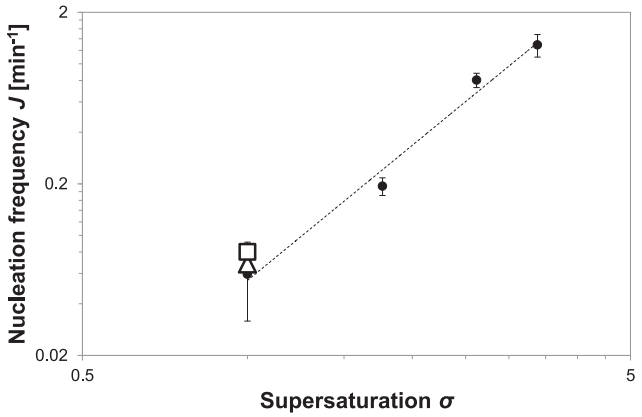


**FIG. 5.** Nucleation frequency $J$ at a range of supersaturations $\sigma$ during the experiment of $CH_4 + C_3H_8$ (90:10) mixed-gas hydrate formation using various water samples (PW: ●, DW: △, and UW: □). The error bars show the standard error of fitting of Eq. (1). Note that data for PW (including the fitting line) are the same as in Fig. 3.

$R^*$ and $\Delta G(R^*)$, which would increase $J$ under the same σ condition. However, the introduction of a more active nucleation site for gas hydrates in water would be expected to increase the nucleation rate by orders of magnitude,[36] not just the tens of percent found here. Thus, we argue that this mechanism does not explain our results. So, we now examine the guest-molecule-buffer mechanism.

Uchida *et al.*[37] showed that the dissolved oxygen ($O_2$) concentration (DO) in $O_2$-UFB containing water at atmospheric pressure kept more than double its saturation value for several days. This effect is thought to result from the high internal pressure of UFBs. Thus, they may act as a buffer of gas molecules in aqueous solution. Under the present experimental conditions, however, UFBs seem to increase the effective supersaturation by at most 16%, much less than that found for the dissolved $O_2$ case above. Therefore, based on the experimental result that the promoting effect of UFBs on the gas hydrate nucleation is smaller than that of $\sigma$, we should either re-evaluate the assumptions in these mechanisms or look for a different mechanism entirely.

Therefore, if one wants to promote the nucleation of the mixed-gas hydrate, increasing $P_0$ to increase $\sigma$ is more effective than using UW or DW. Following the trend in Fig. 5, if $\sigma$ is reduced to about 0.5, the value of $J$ is expected to be nearly one order of magnitude smaller. In addition, since we use a stirring system to form the hydrate, the promotion effect of stirring may overwhelm that from the UFBs. In future studies, to better understand the role of UFBs on $J$, we should examine the $\sigma$ dependence of $J$ with UW and DW, particularly at lower supersaturations.

## IV. CONCLUSIONS

We formed a $CH_4 + C_3H_8$ (90:10) mixed-gas hydrate at $T$ = 274.2 K and a range of initial pressures $P_0$, from 1.1 to 2.5 MPa, to investigate the nucleation probability distribution by measuring the induction time ($t_{ind}$) changes. Here, the driving force is the initial supersaturation $\sigma = P_0/P_d - 1$ ($P_d$: dissociation pressure of this mixed-gas hydrate at $T$). As a result, $t_{ind}$ varied from 5 to 360 min when $\sigma$ = 1.0 with pure water. The resulting nucleation probability distribution of this mixed-gas hydrate was closer to that of pure $CH_4$ hydrate than that of pure $C_3H_8$ hydrate, having a significantly shorter $t_{ind}$ than the latter at roughly the same supersaturation $\sigma$. Therefore, we conclude that increasing the supersaturation significantly shortened the induction period and promoted nucleation. Based on the probability distributions, we found that the calculated nucleation frequency has a power-law relation to supersaturation $\sigma$.

We also examined a method to promote nucleation using water containing ultrafine bubbles (UFBs) as the source water, a method that had previously been found effective for single-gas hydrates.[21–24] We confirmed that, as with the single-gas cases, the UFB-containing water prepared using a generator (UW) has a similar nucleation-promoting effect as the hydrate dissociated water (DW) for this mixed-gas hydrate. Quantitatively, the influence of UFBs in the source water on the promotion of gas-hydrate nucleation at $\sigma$ = 1.0 was found to be equivalent to an increase in supersaturation of only 9%–16%. To better understand these results, we plan to run experiments with UFBs at lower supersaturations.

## ACKNOWLEDGMENTS

This work was partly supported financially by the University Research Support Program of Hokkaido Gas Co., Ltd. and the Arai Foundation. We would like to thank Professor A. K. Sum, Colorado School of Mines, for providing the numerical data of the experiments[34] in the previous work[30] and for his fruitful discussion. The distribution measurements of UFBs were supported by Professor K. Kimura, Mr. S. Kiuchi, and Mr. H. Fernandes (Hokkaido Univ.). The authors also acknowledge the fruitful discussion in the Joint Research Program of the Institute of Low Temperature Science, Hokkaido University (23S002). We would also like to thank Dr. J. Nelson, the editor of Redmond Physical Sciences (www.redmondphysicalsciences.com), for the English language review.

## AUTHOR DECLARATIONS

### Conflict of Interest

The authors have no conflicts to disclose.

### Author Contributions

**Tsutomu Uchida**: Conceptualization (lead); Data curation (lead); Formal analysis (lead); Funding acquisition (lead); Investigation (supporting); Methodology (lead); Resources (lead); Supervision (lead); Validation (lead); Writing – original draft (lead); Writing – review & editing (equal). **Ren Sugibuchi**: Data curation (lead); Formal analysis (lead); Investigation (lead); Writing – review & editing (equal). **Masato Hayama**: Data curation (supporting); Formal analysis (supporting); Investigation (supporting); Writing – review & editing (equal). **Kenji Yamazaki**: Conceptualization (supporting); Methodology (supporting); Supervision (supporting); Validation (supporting); Writing – original draft (supporting); Writing – review & editing (equal).

## DATA AVAILABILITY

The data that support the findings of this study are available from the corresponding author upon reasonable request.

## NOMENCLATURE

| | |
|---|---|
| CSMHYD | the name of the software that predicts the thermodynamics of stable hydrate structures under given pressure, temperature, and composition conditions |
| DW | hydrate dissociated water |
| FFT method | freeze fracture replica method via TEM |
| PW | pure water |
| TEM | transmission electron microscopy |
| UFB | ultrafine bubble |
| UW | UFB-containing water prepared using a UFB generator |

## REFERENCES


[1]A. Vysniauskas and P. R. Bishnoi, "A kinetic study of methane hydrate formation," Chem. Eng. Sci. **38**(7), 1061 (1983).

[2]A. Vysniauskas and P. R. Bishnoi, "Kinetics of ethane hydrate formation," Chem. Eng. Sci. **40**(2), 299 (1985).

[3]P. Englezos, N. Kalogerakis, P. D. Dholabhai, and P. R. Bishnoi, "Kinetics of formation of methane and ethane gas hydrates," Chem. Eng. Sci. **42**(11), 2647 (1987).

[4]P. Englezos, N. Kalogerakis, P. D. Dholabhai, and P. R. Bishnoi, "Kinetics of gas hydrate formation from mixtures of methane and ethane," Chem. Eng. Sci. **42**(11), 2659 (1987).

[5]P. Englezos, N. Kalogerakis, P. R. Bishnoi, and P. R. Bishnoi, "Formation and decomposition of gas hydrates of natural gas components," J. Inclusion Phenom. Mol. Recognit. Chem. **8**, 89 (1990).

[6]P. R. Bishnoi and V. Natarajan, "Formation and decomposition of gas hydrates," Fluid Phase Equilib. **117**, 168 (1996).

[7]M. B. Malegaonkar, P. D. Dholabhai, and P. R. Bishnoi, "Kinetics of carbon dioxide and methane hydrate formation," Can. J. Chem. Eng. **75**, 1090 (1997).

[8]J. Dong Lee, R. Susilo, and P. Englezos, "Methane–ethane and methane–propane hydrate formation and decomposition on water droplets," Chem. Eng. Sci. **60**, 4203 (2005).

[9]E. D. Sloan and C. A. Koh, *Clathrate Hydrates of Natural Gases*, 3rd ed. (CRC Press, Boca Raton, 2007), p. 721.

[10]J. A. Ripmeester, "Improving our understanding of gas hydrate formation processes: The importance of multi-technique approaches," in *Physics and Chemistry of Ice*, edited by W. F. Kuhs (RSC Publishing, Cambridge, UK, 2007), pp. 59–71.

[11]C. P. Ribeiro and P. L. C. Lage, "Modelling of hydrate formation kinetics: State-of-the-art and future directions," Chem. Eng. Sci. **63**, 2007 (2008).

[12]R. Kumar, P. Linga, I. Moudrakovski, J. A. Ripmeester, and P. Englezos, "Structure and kinetics of gas hydrates from methane/ethane/propane mixtures relevant to the design of natural gas hydrate storage and transport facilities," AIChE J. **54**(8), 2132 (2008).

[13]T. P. Sampaio, F. W. Tavares, and P. L. C. Lage, "Non-isothermal population balance model of the formation and dissociation of gas hydrates," Chem. Eng. Sci. **163**, 234 (2017).

[14]S. Maghsoodloo Babakhani, B. Bouillot, J. Douzet, S. Ho-Van, and J. M. Herri, "A new approach of studying mixed gas hydrates involving propane at non-equilibrium conditions and final state: An experimental study and modeling," Chem. Eng. Sci. **179**, 150 (2018).

[15]W. Ke, T. M. Svartaas, and D. Chen, "A review of gas hydrate nucleation theories and growth models," J. Nat. Gas Sci. Eng. **61**, 169 (2019).

[16]P. Englezos, S. Alavi, and J. A. Ripmeester, "Kinetics of clathrate hydrate processes," in *Clathrate Hydrates: Molecular Science and Characterization*, edited by J. A. Ripmeester and S. Alavi (Wiley-VCH GmbH, Weinheim, Germany, 2022), Vol. 2, pp. 631–716.

[17]V. Natarajan, P. R. Bishnoi, and N. Kalogerakis, "Induction phenomena in gas hydrate nucleation," Chem. Eng. Sci. **49**(13), 2075 (1994).

[18]D. Kashchiev and A. Firoozabadi, "Nucleation of gas hydrates," J. Cryst. Growth **243**, 476 (2002).

[19]D. Kashchiev and A. Firoozabadi, "Induction time in crystallization of gas hydrates," J. Cryst. Growth **250**, 499 (2003).

[20]M. Khurana, Z. Yin, and P. Linga, "A review of clathrate hydrate nucleation," ACS Sustainable Chem. Eng. **5**, 11176 (2017).

[21]T. Uchida, R. Sugibuchi, K. Yamazaki, and K. Gohara, "Nucleation behavior of single-gas hydrates in the batch-type stirred reactor and their promotion effect with ultrafine bubbles: A mini review and perspectives," Energy Fuels **36**, 10444 (2022).

[22]T. Uchida, K. Yamazaki, and K. Gohara, "Gas nanobubbles as nucleation acceleration in the gas-hydrate memory effect," J. Phys. Chem. C **120**(47), 26620 (2016).

[23]T. Uchida, H. Miyoshi, R. Sugibuchi, A. Suzuta, K. Yamazaki, and K. Gohara, "Contribution of ultra-fine bubbles to promoting effect on propane hydrate formation," Front. Chem. **8**, 480 (2020).

[24]T. Uchida, H. Miyoshi, K. Yamazaki, and K. Gohara, "Promoting effect of ultra-fine bubbles on $CO_2$ hydrate formation," Energies **14**, 3386 (2021).

[25]B. Kvamme, S. A. Aromada, N. Saeidi, T. Hustache-Marmou, and P. Gjerstad, "Hydrate nucleation, growth, and induction," ACS Omega **5**, 2603 (2020).

[26]T. Uchida, K. Yamazaki, and K. Gohara, "Generation of micro- and nano-bubbles in water by dissociation of gas hydrates," Korean J. Chem. Eng. **33**(5), 1749 (2016).

[27]E. D. Sloan and F. A. Fleyfel, "A molecular mechanism for gas hydrate nucleation from ice," AIChE J. **37**(9), 1281 (1991).

[28]B. J. Falabella, "A study of natural gas hydrates," Ph.D. thesis, University of Massachusetts, Amherst, MA, 1975.

[29]P. Skovborg, H. J. Ng, P. Rasmussen, and U. Mohn, "Measurement of induction times for the formation of methane and ethane gas hydrates," Chem. Eng. Sci. **48**(3), 445 (1993).

[30]D. É. S. de Menezes, A. K. Sum, A. Desmedt, P. d. A. Pessôa Filho, and M. D. Robustillo Fuentes, "Coexistence of sI and sII in methane–propane hydrate former systems at high pressures," Chem. Eng. Sci. **208**, 115149 (2019).

[31]E. D. Sloan, Jr., "Clathrate hydrates of natural gases," in *Revised and Expanded*, 2nd ed. (CRC Press, Boca Raton, FL, 1998), p. 705, DOS version of CSMHYD program is available on http://hydrates.mines.edu/CHR/Software.html.

[32]S. Toschev, A. Milchev, and S. Stoyanov, "On some probabilistic aspects of the nucleation process," J. Cryst. Growth **13–14**, 123 (1972).

[33]S. Takeya, A. Hori, T. Hondoh, and T. Uchida, "Freezing-memory effect of water on nucleation of $CO_2$ hydrate crystals," J. Phys. Chem. B **104**, 4164 (2000).

[34]A. K. Sum, personal communication (2022).

[35]S. Karthika, T. K. Radhakrishnan, and P. Kalaichelvi, "A review of classical and nonclassical nucleation theories," Cryst. Growth Des. **16**, 6663 (2016).

[36]M. Rahmati-Abkenar, M. Manteghian, and H. Pahlavanzadeh, "Experimental and theoretical investigation of methane hydrate induction time in the presence of triangular silver nanoparticles," Chem. Eng. Res. Des. **120**, 325 (2017).

[37]T. Uchida, S. Liu, M. Enari, S. Oshita, K. Yamazaki, and K. Gohara, "Effect of NaCl on the lifetime of micro- and nanobubbles," Nanomaterials **6**, 31 (2016).